

STRUCTURE AND DYNAMICS OF NANOCOMPOSITE POLYMER ELECTROLYTES

E. MANIAS, A.Z. PANAGIOTOPOULOS, D.B. ZAX AND E.P. GIANNELIS

CONTENTS	185
INTRODUCTION	186
EXPERIMENTAL	189
Materials	189
Materials	189
IONIC CONDUCTIVITY OF PEO NANOCOMPOSITES	191
COOPERATIVE MOTION: TSC AND DSC	192
LOCAL CHAIN DYNAMICS: NMR	195
COMPUTER SIMULATIONS OF NANOCOMPOSITES	196
CONCLUSIONS	203
ACKNOWLEDGEMENT	203
REFERENCES	203

STRUCTURE AND DYNAMICS OF NANOCOMPOSITE POLYMER
ELECTROLYTES

E. MANIAS

A.Z. PANAGIOTOPOULOS

D.B. ZAX

and

E.P. GIANNELIS

INTRODUCTION

Improvements in rechargeable, high-energy density batteries are essential for the development of products ranging from zero-emission vehicles to portable electronics. Batteries based on polymer electrolytes are the subject of active R&D competition worldwide. A key unsolved problem is the design and implementation of lightweight, chemically stable and environmentally benign electrolyte/electrode combinations. Of particular interest are Li⁺ salts dissolved in flexible polymers like poly(ethylene oxide), PEO, since these systems combine promisingly high ionic conductivities with processability and are conveniently interfaced to high energy density Li electrodes. A serious drawback in these systems has been the precipitous decrease of conductivity (from 10⁻⁴ to 10⁻⁸ S/cm) at temperatures below the melting temperature, which occurs usually above room temperature. This decrease is due to the formation of crystallites in the polymer matrix that severely impede ionic mobility.

One of the most promising ways to improve the electrochemical performance of polymer electrolytes is by the addition of inorganic fillers (Skaarup et al., 1980; Wiczonek, 1992; Capuano et al., 1991). The resulting composite polymer electrolytes (CPE) display enhanced conductivity, mechanical stability and improved interfacial stability towards electrode materials. Despite the improved properties of CPE, however, their application in rechargeable lithium batteries is still hindered by low ionic conductivity at ambient temperature, low lithium transport number and difficulties in processing.

Polymer nanocomposites represent an alternative to conventional CPE. Because of the significantly reduced phase dimensions of the inorganic and the polymer matrix (1-100 nm), nanocomposites often exhibit new and improved properties, when compared to their macrocomposite counterparts (i.e. filled polymers). One promising way to synthesize polymer nanocomposites is by intercalating polymers in layered inorganic hosts (Vaia, et al., 1995; Wong et al., 1995; Wong et al., 1996; Mehrotra and Giannelis, 1991; Kanatzidis et al., 1989; Kanatzidis et al., 1989; Cao and Mallouk, 1991; Pillion et al., 1991; Divigalpitiya et al., 1991; Nazar et al., 1992; Messersmith and Stupp, 1992; Aranda and Ruiz-Hitzky, 1990; Aranda and Ruiz-Hitzky, 1992; Aranda and Ruiz-Hitzky, 1994; Wu, and Lerner, 1993; Aranda and Ruiz-Hitzky, 1990; Hutchinson et al., 1996; Vaia et al., 1997). Graphite, transition metal chalcogenides and 2:1 phyllosilicates are some examples of layered solids capable of intercalation. The structure and properties of the resulting nanostructures can be conveniently mediated by controlling subtle guest-host interactions.

A promising group of candidates for polymer intercalation are layer silicates from the smectite group, which share the same structural characteristics as the better-known talc and mica (Grim, 1953). Their crystal lattice consists of layers made up of two silica tetrahedral sheets fused to an edge-shared octahedral sheet of nominally aluminum or magnesium oxide. Stacking of the layers leads to a regular van der Waals gap between the layers. In talc the layers are electrically neutral. In contrast, the silicate layers in mica and the smectite group are anionically charged and the charge is balanced by alkali or alkaline earth cations that typically reside in the galleries between the layers. Because of the relatively weak bonding between the layers intercalation of small molecules and even polymers between the layers is facile in smectites.

There are two particular aspects that we exploit in designing polymer electrolytes by intercalation of polymers in phyllosilicates (Fig. 1). First, polymer intercalation disrupts the normal, three-dimensional structure of the polymer chains and offers a means to suppress the polymer crystallization. Furthermore, since the counter anions are the relatively large silicate layers as compared to the traditionally used salts (e.g. ClO_4^- , CF_3SO_2^-), single ionic

behavior is expected. These two new features allow us to molecularly engineer the electrolytes so as to preferentially retain desirable while suppressing the undesirable properties.

In this chapter we combine experiments and computer simulations to study the structure and dynamics of PEO nanocomposite electrolytes. From these studies a new and quite unexpected picture for the nanocomposite electrolytes is emerging. The cations are still pinned to the silicate host surface while the intercalated polymer chains adopt a disordered, random configuration inside the host galleries. Despite the presence of the “confining” host layers, the intercalated PEO chains exhibit substantial segmental motion even at temperatures well below the bulk glass transition temperature.

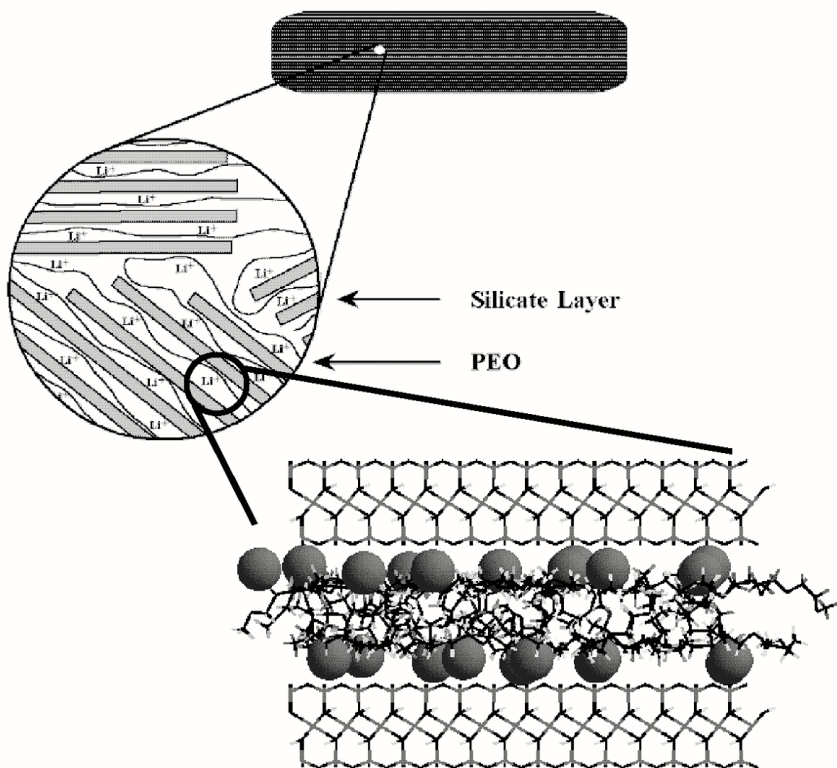


Figure 1. Idealized structure of intercalated polymer/mica-type layered silicate nanocomposites at different length scales.

EXPERIMENTAL

Materials

Na-montmorillonite with a cation exchange capacity of 85 meq/100 g and an idealized unit cell formula of $\text{Na}_{0.67}[\text{Al}_{3.33}\text{Mg}_{0.67}]\text{Si}_8\text{O}_{20}(\text{OH})_4$ was obtained from the Source Clay Mineral Repository, University of Missouri. The mineral was allowed to sediment 24 hrs as a 1 wt% aqueous slurry to remove impurities, saturated with Na^+ or Li^+ by reaction with excess aqueous NaCl or LiCl, respectively, washed free of chloride by dialysis, and then dried.

Li-fluorohectorite is a synthetic hectorite in which the octahedral lattice hydroxyl groups are replaced with fluoride ions, and its unit cell is $\text{Li}_{1.6}[\text{Mg}_{4.44}\text{Li}_{1.6}]\text{Si}_8\text{O}_{20}\text{F}_4$. This phyllosilicate has a typical particle size ~ 5 microns and a cation exchange capacity of 190 meq/100 g, and was obtained from Corning Inc.

Nanocomposites were prepared by either solution or melt intercalation. The solution intercalates were prepared as described previously by suspending Li-montmorillonite (Li exchanged SWy-1, University of Missouri Clay Repository) or Li-fluorohectorite (Corning Inc.) in de-ionized water and subsequently adding the suspension to an aqueous solution of 4% PEO ($M_w=100,000$, PolySciences)(Aranda and Ruizitzky, 1992; Wu and Lerner, 1993). The mixture was stirred for 12 hours and the resulting product was washed three times with de-ionized water. Moderately flexible films of the solution intercalated hybrid were formed by re-suspending the washed product in de-ionized water and casting the suspension on glass plates to dry. Thermal gravimetric analysis (TGA) indicated that the hybrid contained ~ 25 wt.% PEO. X-ray diffraction of the films show an ordered multilayer structure with a repeat unit of 1.77 nm, indicating that the intercalated PEO occupies an interlayer space of only 0.82 nm (silicate layer thickness ~ 0.95 nm Grim, 1953).

Melt intercalates were made by blending powders of Li-montmorillonite or Lifuorohectorite and PEO in the desired weight ratio, cold pressing the admixture into a pellet, and annealing at 80 °C for 10 hours (Vaia et al., 1995). The resulting pellet was reground and reannealed under similar conditional three more times to ensure complete polymer intercalation. X-ray diffraction of the powders was the same as that from the solution intercalates ($d_{(001)} = 1.77$ nm).

Typical samples for TSC and DSC were nominally 0.2 mm thick with area greater than 5 mm². The moderately flexible films obtained from solution intercalation were cut into the appropriate size. For the melt intercalates, disks were formed using a hydraulic press (70 MPa) and subsequently cut to size. Control samples of pristine silicate were cast from water or formed into pellets.

Materials

Standard "global" TSC scans were obtained using a Solomat 41000 (Stamford, CT) and previously outlined procedures (Vaia et al., 1997; Sauer and Avakian, 1992). In general, the sample was heated to a polarization temperature (T_p) which is usually well above the glass transition temperature of the polymer (T_g) and quenched at 30°C/minute under an applied electric field of $E \sim 1000 \text{ kV/m}$. After removing the field, the film is shorted across an electrometer to measure the depolarization current as the sample is heated at 7°C/min. Global TSC spectra are roughly comparable to low frequency (ca. 10^{-3} Hz) dielectric loss spectra. Discretion must be applied in interpreting the spectra, especially for relaxations above the glass transition region, because these features are generally not related to polymer motions, but are due to electrode polarization or charge migration effects in the near electrode region.

Thermal sampling (TSC-TS) spectra are obtained by applying the electric field, E , for two minutes over a narrow temperature window from T_p to $T_p - 5^\circ\text{C}$. The field is removed and the sample is held for an additional two minutes at $T_p - 5^\circ\text{C}$. It is then quenched to about 40°C below T_p . The depolarization spectrum due to a narrow distribution of relaxations associated with the hold temperature is measured in a manner similar to the global TSC experiment by heating at 7°C/min to about 30°C above T_p . The procedure is repeated for each chosen T_p . The TSC-TS spectra are analyzed as described previously to obtain activation energy related to the relaxation processes at the hold temperatures (Vaia et al., 1997; Sauer and Avakian, 1992). DSC data were collected on a Perkin Elmer and a T.A. 9900 thermal analysis station.

Solid state NMR experiments were carried out in a 7.05 Tesla wide bore superconducting magnet equipped with a laboratory built, broad band Fourier transform pulse spectrometer and probes. Variable temperature experiments were conducted in a continuous flow cryostat (Oxford Instruments CF-1200). ^2H NMR spectra were acquired with quadrupolar echo sequences, while ^7Li spectra were acquired with spin-echo sequences.

Ionic conductivity of PEO nanocomposites was determined from ac impedance measurements. Pellets were evacuated at 100°C before sandwiching between two metal lithium electrodes. To minimize moisture interference samples were prepared and loaded into sealed electrochemical cells in a drybox. ac ionic conductivity was calculated from the complex impedance plot using nonlinear computer fitting.

IONIC CONDUCTIVITY OF PEO NANOCOMPOSITES

An Arrhenius plot of the in-plane ionic conductivity of the PEO/Li⁺-montmorillonite nanocomposite containing 40 wt% polymer is shown in Figure 2. For comparison, the conductivity of a conventional LiBF₄/PEO electrolyte with a comparable Oxygen/Li ratio is also shown. As expected the conductivity of the LiBF₄/PEO electrolyte decreases sharply, by several orders of magnitude, below the melting temperature. In contrast, the conductivity of the nanocomposite exhibits only weak temperature dependence over the same temperature range. In addition, the apparent activation energy in the nanocomposite (2.8 kcal/mol) is of the same order of magnitude to that of the molten polymer electrolyte, suggesting that the mobility of Li⁺ in the nanocomposites is comparable to that in the bulk molten electrolyte. Furthermore, the out-of-plane conductivity of the hybrid is only an order of magnitude lower from the in-plane conductivity.

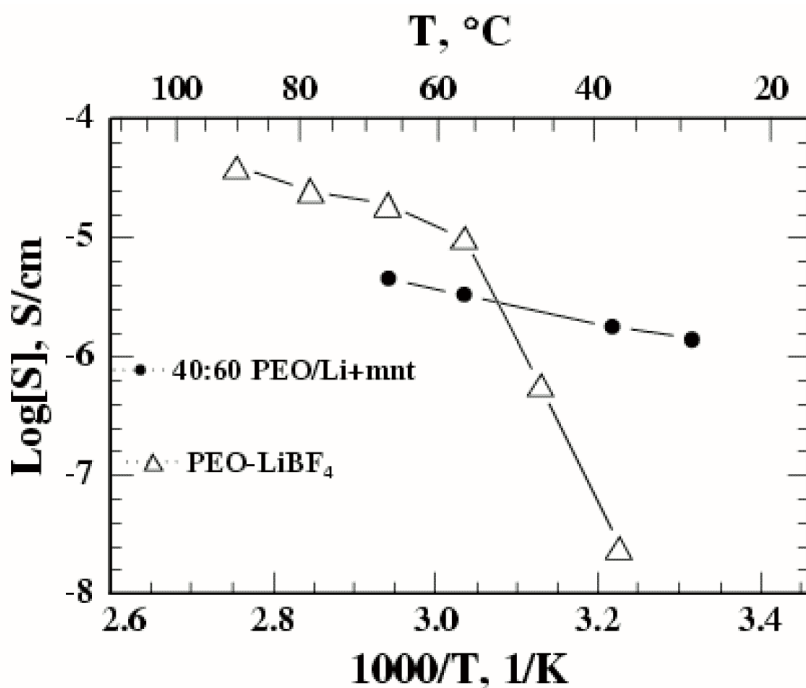


Figure 2. Arrhenius plots of the ionic conductivity for a bulk LiBF₄-PEO system and an intercalated PEO/Li⁺ montmorillonite nanocomposite (from Vaia et al., 1995).

The conductivity of the melt-intercalated hybrid is much higher and more isotropic than that reported previously for PEO/silicate nanocomposites. Note, however, that those samples were prepared by solution intercalation and were thoroughly washed to remove excess polymer (Aranda and Ruiz-Hitzky,

1990; Aranda and Ruiz-Hitzky, 1992; Aranda and Ruiz-Hitzky, 1994; Wu and Lerner, 1993). The enhanced ionic conductivity in our samples is probably due to the presence of excess polymer (40 vs. 30 wt.%) that provides an easy conduction path between host particles. Removing excess polymer could lead to chain depletion from the edges of the silicate particles hindering the interparticle mobility of Li^+ ions. Furthermore, the tendency of silicate particles to orient parallel to the film surface when processed from solution is minimized in the dry-pressed samples used in this study leading to more isotropic properties.

The high ionic conductivity due to the increased amorphization of the polymer is entirely due to the mobile Li^+ cations, as the counter anions in the nanocomposites are the very large silicate layers, with particle diameters of ~ 1 micron. The simplified chemistry of interfacing to single ion conductor overcomes another of the major limitations of conventional polymer electrolytes and makes the nanocomposites a promising alternative for further development.

COOPERATIVE MOTION: TSC AND DSC

The presence of cooperative motion of chain segments along the intercalated polymer chains may be examined using various analytical techniques such as DSC, TSC, and dielectric spectroscopy. Figure 3 shows the characteristic thermal behavior of bulk PEO. The large endotherm at 66°C corresponds to melting of crystalline regions of PEO whereas the step in the trace at -55°C corresponds to the bulk glass transition. Over this temperature range (-70 - 150°C), the silicate does not exhibit any thermal transitions. Thus assuming the thermal responses are additive, events observed in the DSC for the PEO nanocomposites are entirely related to the thermal behavior of the polymer. To eliminate the influence of water, samples were dried in vacuum at 100 - 150°C overnight.

For the melt intercalated samples, no thermal events were observable. Confinement of the polymer chains between the silicate layers effectively prohibits bulk-like crystallization. The absence of PEOs melting transition ($T_m = 66^\circ\text{C}$) indicates that essentially all the polymer is intercalated. No evidence of the glass transition, which is clearly seen in pure PEO at -55°C (Figure 3) by DSC, was found in the nanocomposite. If one exists, it is too weak or too broad to be detected by DSC. In general, DSC is probably not sensitive enough to detect any weak transitions of the intercalated polymer, and the low volume fraction of polymer makes the sensitivity even worse.

Thermally stimulated current techniques have enhanced sensitivity to cooperative relaxations such as glass transitions. To further evaluate the glass transition region of the intercalated PEO, TSC was applied in two modes-

“global” and “thermal sampling”. As with the DSC, no clear peak was observable in the global TSC spectra of the intercalated PEO in the temperature range of the bulk glass transition. Thus, cooperative relaxations of the intercalated polymer are, at best, weak.

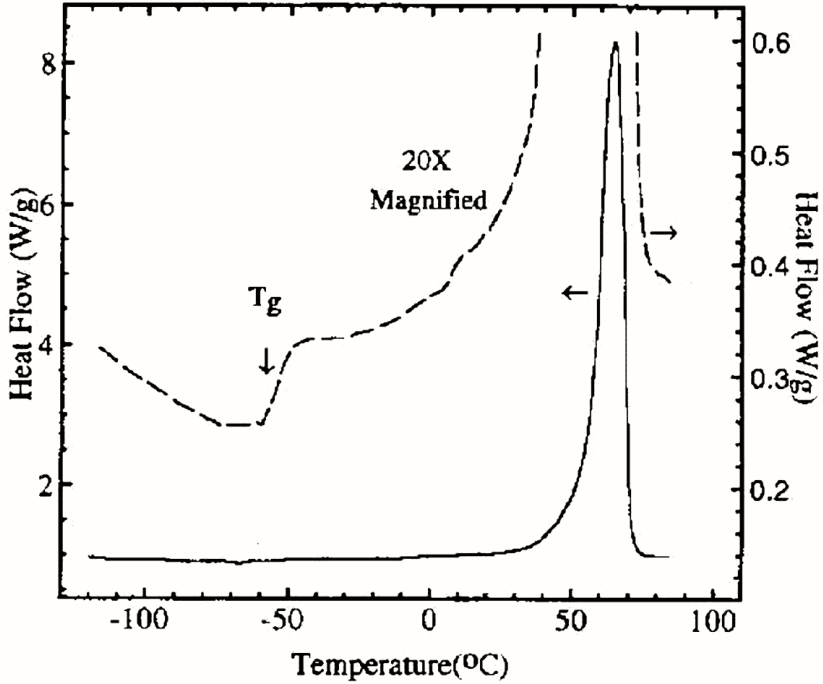


Figure 3. DSC heating run (40°C/min) for 100% PEO (from ref 22).

Thermally stimulated current measurements with thermal sampling are sensitive to cooperative relaxations from a minor fraction of the overall relaxing species. The apparent activation energies, E_a , of relaxations contributing to the depolarization current for neat PEO, the nanocomposite containing 20% PEO, and a montmorillonite control pellet are shown in Figure 4. The analysis consists of assigning cooperative glass transition like motions to the regions of departure of the values of E_a from the $\Delta S^\ddagger = 0$ prediction using:

$$E_a = \Delta H^\ddagger + RT = RT [22.92 + \ln(T/f)] + T \Delta S^\ddagger \quad (1)$$

where ΔH^\ddagger and ΔS^\ddagger are the activated states enthalpy and entropy, respectively, and f is the frequency (Vaia et al., 1997; Sauer and Avakian, 1992). Equation 1 was derived by rearranging Eyring's activated states equation (Boek et al., 1995) and can be used to predict values of E_a with no adjustable

parameters by setting the activated states entropy (ΔS^\ddagger) equal to zero. For the PEO intercalate a distinct peak in E_a is not observed and in fact a broad transition starting at about the nominal PEO T_g and ranging up to about 60°C is observed.

Of the many systems studied with the TSC-TS technique, *never* before has such broad transition region with a low degree of cooperatively been observed. On the basis of the data in Figure 4, we conclude that the motions of the intercalated PEO chains are inherently non-cooperative relative to the cooperative T_g motions in less unconstrained environments such as for amorphous chains confined between crystal lamellae in pure semi-crystalline PEO. For semi crystalline PEO, the chains are confined in "amorphous" gaps a few nanometers wide whereas the intercalated PEO occupies a gap of less than one nanometer.

Taken in context with previous investigations of polymer relaxations in confined environments, the results from the intercalated PEO appear to indicate that cooperative motion precipitously decreases as polymers are confined to extremely narrow slits less than a few nanometers.

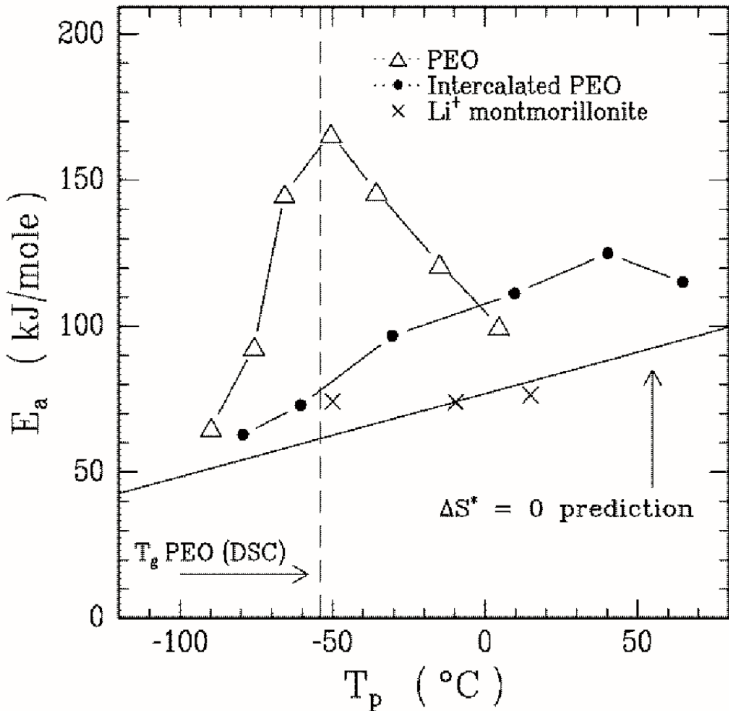


Figure 4. Temperature dependence of the apparent activation energies (E_a) as determined by TSC measurements with thermal sampling for 20 wt % intercalated PEO in montmorillonite, pure PEO and pure montmorillonite. The departure of E_a from the $\Delta S^\ddagger=0$ prediction indicates the glass transition region.

LOCAL CHAIN DYNAMICS: NMR

The local dynamics of intercalated chains of PEO were probed using solid-state NMR. Figure 5 compares the ^2H line shapes for bulk *d*-PEO ($M_w = 180000$, $M_w/M_n = 1.2$, Polysciences) and intercalated *d*-PEO in Li-fluorohectorite.

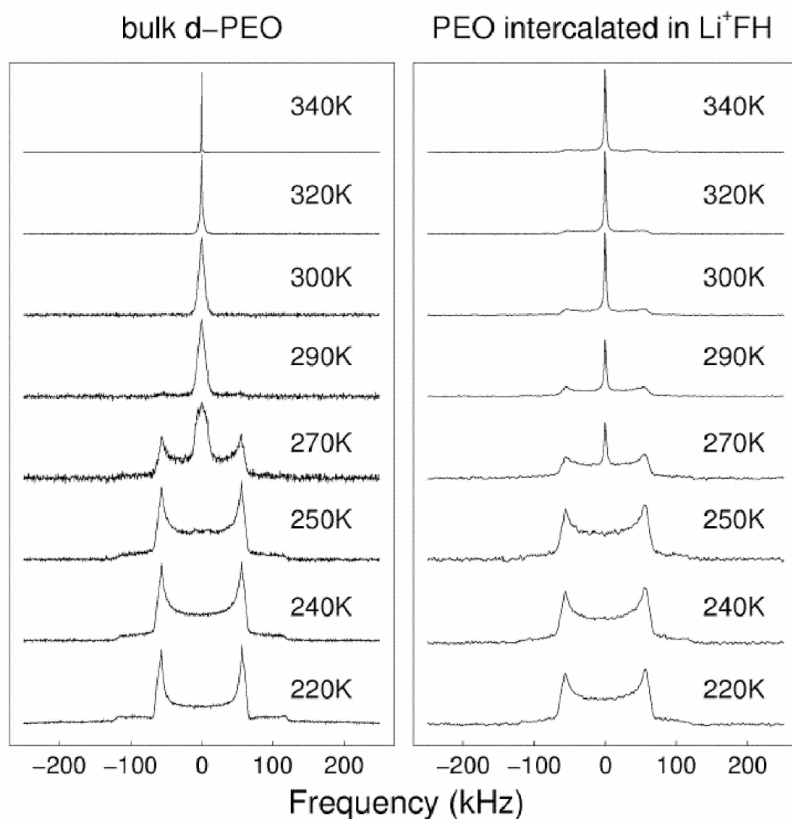


Figure 5. Comparison of ^2H NMR line shapes of bulk *d*-PEO and Li-fluorohectorite intercalated *d*-PEO, as a function of temperature.

At low temperature, where the local segmental motion of the polymer is quiescent, a typical powder pattern is observed for both the bulk *d*-PEO and the intercalated *d*-PEO, indicating the spatial motion of the deuterium is slower than the time scale of the experiment. However, as the temperature increases, a *narrow* central peak develops at lower temperatures for the intercalated *d*-PEO than for the bulk polymer. Additionally, the breadth of the central peak from the intercalated *d*-PEO is substantially narrower than that of the bulk polymer. This

central peak results from increased segmental motion, which causes temporal averaging of the signal. The temperature dependence of the line shapes indicates that the intercalated chains have more “freedom” to sample a distribution of local chain configurations, resulting in increased signal averaging. However, at the highest temperatures, the intercalated *d*-PEO still exhibits a broad base structure reminiscent of the powder pattern, whereas the bulk polymer shows complete motional narrowing of the signal. This indicates that even though the local segmental motion of the intercalated *d*-PEO appears more dynamic at lower temperatures, the silicate layers still restrict motion such that some local configurations of the chain are not accessible, and thus complete signal averaging is not possible.

The linewidth of Li NMR spectra for nanocomposites based on montmorillonite were substantially broader than in the analogous fluorohectorite-based systems. The broadening has been attributed to the presence of paramagnetic Fe³⁺ ions substituting Al³⁺ in the octahedral lattice sites. At low temperatures where no dynamics are found simulations of the expected ⁷Li linewidth and shape suggest that the Li⁺ ions reside along the silicate surface and that the intercalated PEO chains reside primarily towards the middle of the interlayer. Simulations of the NMR spectra provide an average distance between the Li⁺ cations and the Fe³⁺ ions in the octahedral sheet of 0.4 nm, which suggests that the cations are strongly interacting and virtually pinned to the silicate surface. These results contrast with the generally accepted viewpoint, which suggests that PEO mediates the interactions between the cation and the negatively charged silicate surface and draws the cation away from the surface.

COMPUTER SIMULATIONS OF NANOCOMPOSITES

To further probe both the structure and the dynamic behavior of the nanocomposites we have also carried out computer simulations. Atomistic simulations have the ability to “observe” directly both atomistic (for the cation) and molecular (for the polymer) structure and dynamics. Realistic interatomic potentials for the interactions of the silicates with water, alkali cations and polymers are now available and provide useful predictions (Skipper, et al., 1995,; Boek et al., 1995;Deville, 1993; Karaborniet, et al.,1996;Chang et al., 1997; Hackett et al., 1998). Furthermore, these simulations provide a method for making the connection between the microscopic and macroscopic world. In this spirit, progress has been made in concurrent use of Monte Carlo (MC) and Molecular Dynamics (MD) simulations, based on commercial software packages, but with the implementation of force fields that can accurately simulate both pristine and polymer-intercalated silicates.

MC simulations can very efficiently and with moderate computational effort (e.g. on a Pentium-based system in a few hours of CPU time) scan the

relevant phase-space available to these systems and provide the equilibrium thermodynamic state. Parameters such as temperature, pressure, and chemical composition can be easily accommodated and analyzed by MC methods providing structural, conformational and thermodynamic data, which can serve as a sensitive test to our experimentally-derived understanding. On the other hand, dynamic information (e.g. polymer relaxation times and cation mobilities) is available only through Molecular Dynamics simulations. Though the computational demands of such simulations are substantially greater than of MC methods, for small model systems these simulations are accessible, as several nanoseconds of real time need a few CPU-days to be simulated.

Our initial Monte Carlo studies initially focused on the hydrated states of pristine layer silicates and monovalent cations (e.g. Li^+ or Na^+). Although there exist many computer simulations of hydrated silicates in the literature (Skipper et al., 1995; Boek et al., 1995; Deville, 1993; Karaborni et al., 1996; Chang et al., 1997) this approach was necessary to work towards the simulation of intercalated oligomers (Hackett et al., 1998) and polymers (Hackett et al., 2002).

We started by calculating the water uptake in Na-montmorillonite as a function of d-spacing (Fig. 6). Our results agree well with experimental data as well as those obtained by computer simulations by Karaborni et al. (1996).

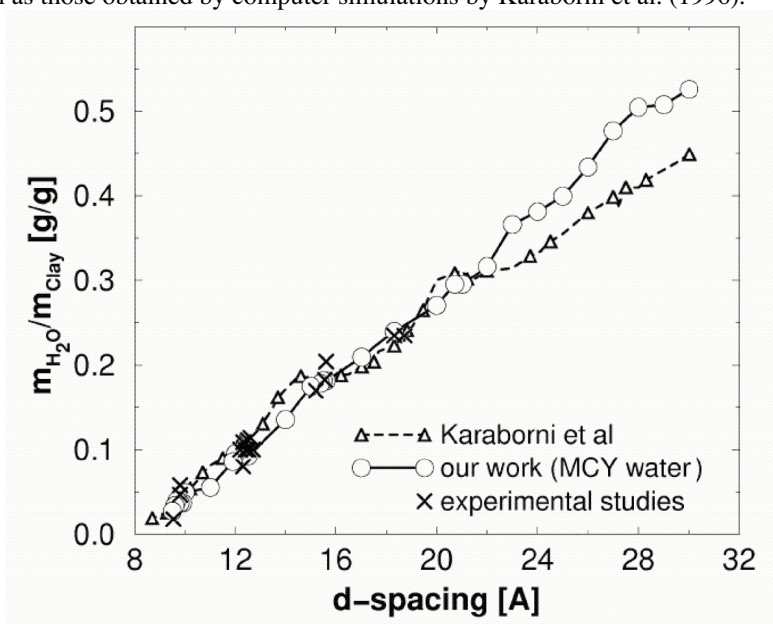


Figure 6. Water uptake of Na-montmorillonite as a function of d-spacing; comparison between our simulation (O) and experimental findings (x).

Beyond the water uptake, the minimized free energy, and the disjoining pressure as functions of d-spacing were also calculated (Fig.7). Four local minima at d-spacing 0.97, 1.21, 1.55 and 1.82nm are seen. These d-spacings correspond to an essentially non-hydrated/collapsed silicate and to structures with one, two, and three layers of water intercalated between the silicate galleries, respectively, in excellent agreement with the experimental data. A decrease in the d-spacing from the value corresponding to a stable hydrated state causes the energy and the disjoining pressure to increase. A gradient of disjoining pressure gives rise to a restoring force, which would bring the system back to the state where both the energy and the disjoining pressure have local minima. On the other hand, if the basal spacing is increased further, so that more water can be adsorbed into the extra room, it will lead finally to an exfoliated state, where the silicate layers are dispersed in water. The minimized free energy is decreasing systematically with increasing basal spacing. Thus, the thermodynamically most favorable state is one with the d-spacing diverging to infinity, which corresponds to completely hydrated clay. The same conclusion can be inferred from the disjoining pressure, which is converging to a zero gradient, thus the system offers no resistance to clay swelling.

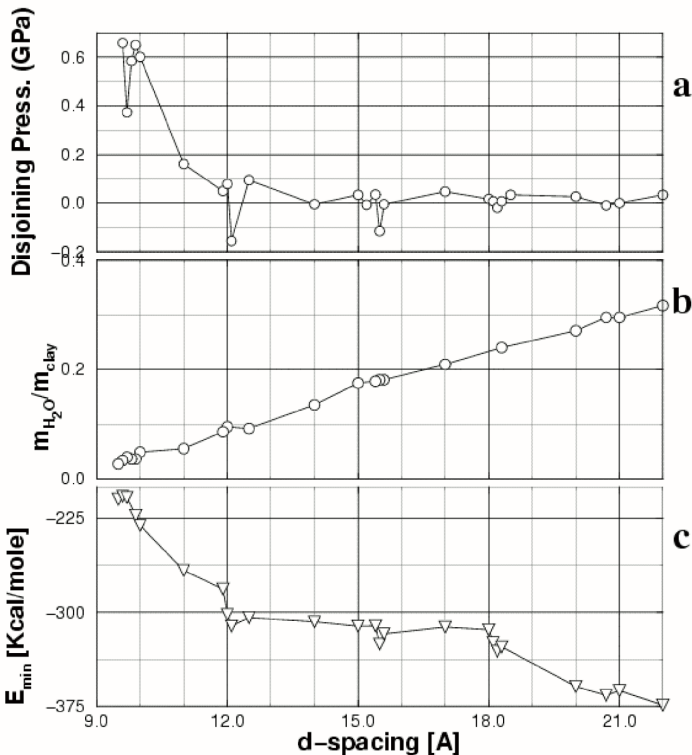


Figure 7. Disjoining pressure (a), water uptake (b) and minimized free energy (c) of a hydrated Na⁺/montmorillonite system as a function of d-spacing.

Complementary Molecular Dynamics simulations have provided a more complete picture of the stable hydrated states obtained above. Starting with the MC simulations as our initial configurations a range of structural and dynamical properties such as density profiles and mean square displacements of both interlayer water and gallery cations were obtained. Figures 8a-8d are snapshots for the four stable hydrated states. When the d-spacing is 0.97 nm all the interlayer water and cations are embedded inside the hexagonal cavity formed by the oxygen atoms on the silicate surface (Fig. 8e). For $d = 1.21, 1.55$ and 1.82 nm the water molecules form one, two, and three layers of water, respectively, inside the silicate galleries. In the collapsed silicates or those containing a monolayer of water the cations are virtually pinned to the silicate surface. Only in the heavily hydrated states are the cations dragged away from the surface and brought towards the middle of the gallery. The layered structure in the silicate gallery that is described above can be readily seen in the density profiles shown in Figure 9.

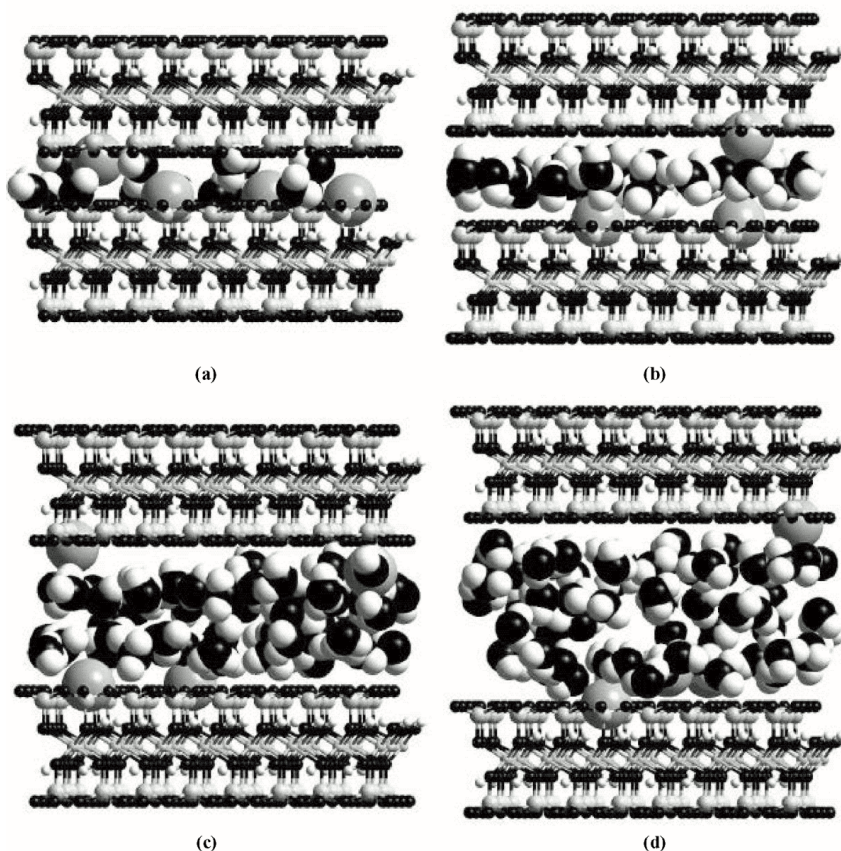


Figure 8. Snapshot of Na-montmorillonite for various hydration levels. The structures of the stable d-spacings are shown: (a) $d=0.97\text{nm}$, (b) $d=1.21\text{nm}$, (c) $d=1.55\text{nm}$, and (d) $d=1.82\text{nm}$.

The mean square displacements of gallery water and Na⁺ cations as a function of time for some of the stable hydrated states are shown in Figure 10. Results from bulk aqueous solution of Na⁺ are included for comparison. As the level of hydration increases the mobility of water and cations in the galleries increases. Interestingly, the mobility of water in the two- and three-layer hydrated state is higher from that in the bulk. Of course the mobility is highly anisotropic with the in-plane diffusivities (parallel to the silicate layers) much higher from those normal to the plane.

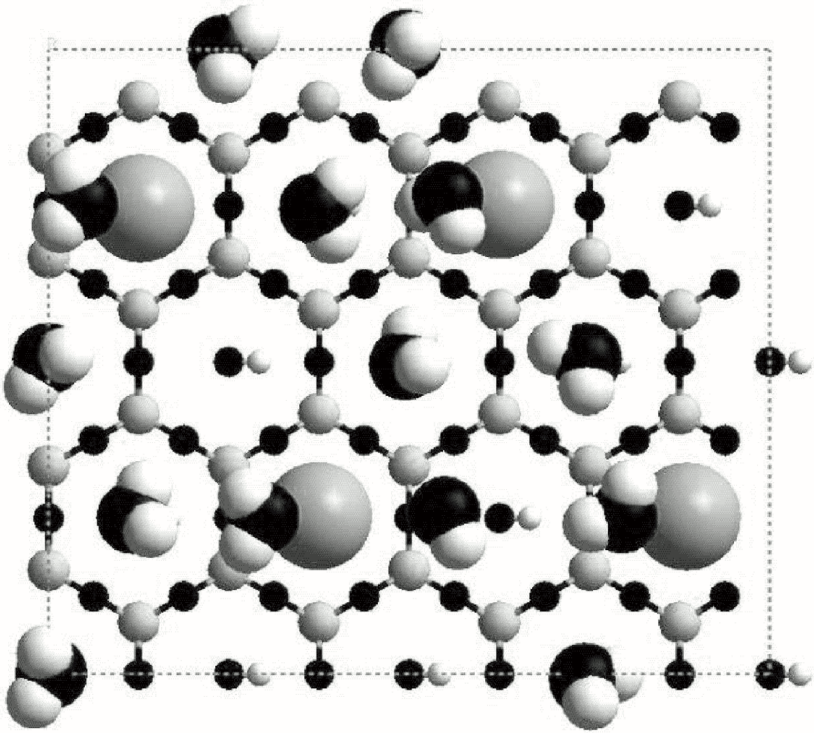


Figure 8. (e) Top view of the interlayer cations and the water molecules for the $d=0.97\text{nm}$ montmorillonite structure. Both Na and H₂O are located inside the surface cavities of the silicates.

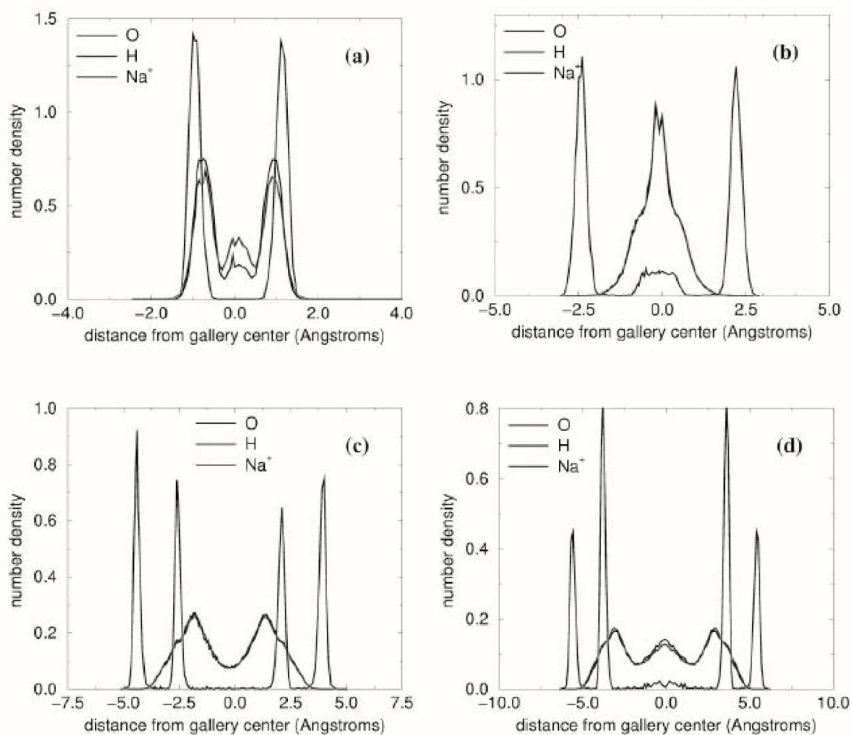


Figure 9. Density profiles for the interlayer water and cations for sodium montmorillonite: (a) 0.97 nm; (b) 1.21 nm, (c) 1.55 nm, and (d) 1.82 nm.

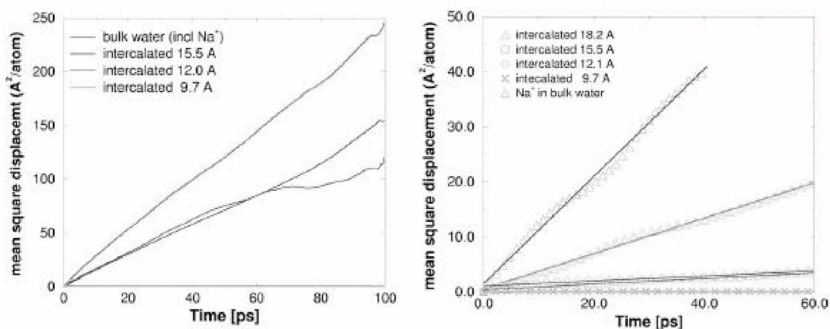


Figure 10. Mean square displacements of water (left) and of Na⁺ (right) in hydrated Na⁺ montmorillonite systems and bulk solution of NaCl in water.

Based on the Einstein relation the self-diffusion coefficients can be calculated from the mean square displacements, and are summarized in Table 1.

Table 1. Diffusion Coefficients for Water Molecules and Cations.

System	Density (g/cm ³)	D _{H₂O}	D _{Na+}
Silicate with one water layer	1.20	1.1x10 ⁻⁵	1.1x10 ⁻⁵
Silicate with two water layers	0.86	3.9x10 ⁻⁵	1.1x10 ⁻⁵
Silicate with three water layers	0.70	7.6x10 ⁻⁵	6.1x10 ⁻⁵
Bulk water (MCYsim)	1.01	2.5x10 ⁻⁵	1.6x10 ⁻⁵
Bulk water (experiment)		2.3x10 ⁻⁵	1.4x10 ⁻⁵

Similar modeling methodologies have provided structural information for the PEO nanocomposites (Fig. 11). In good agreement with the NMR studies the cations are virtually pinned to the silicate layers – i.e. PEO interacts too weakly to drag the cation away from the attractive potential associated with the negatively charged silicate layers. In addition, in both the one- and two-layer intercalated systems the polymer configurations appear largely disordered.

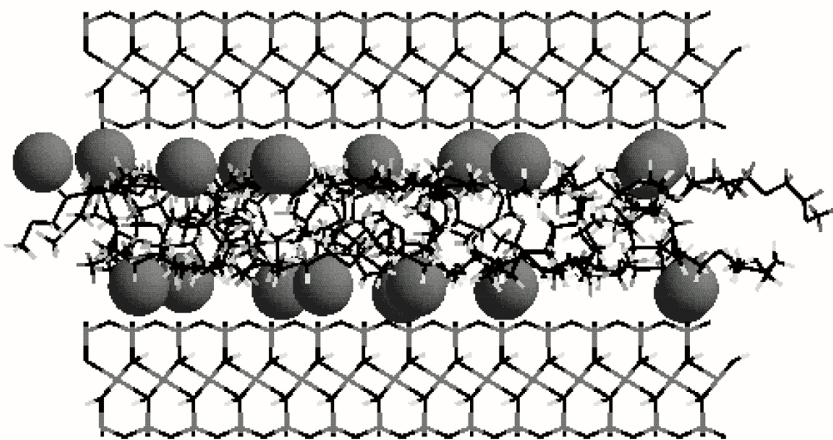


Figure 11. Snapshot of the equilibrium structure of PEO intercalated in Na⁺ montmorillonite, from concurrent MC and MD atomistic simulations.

Our recent neutron scattering experiments support the simulation findings. Peak intensities obtained as a function of diffraction angle are reproduced poorly by any of the models, which have been previously suggested

—such as an extended monolayer and bilayer, or a helical crystalline structure. The neutron scattering experiments instead support a disordered polymer configuration from 15K to room temperature.

CONCLUSIONS

In summary, polymer electrolyte nanocomposites have been synthesized by direct melt and solution intercalation of PEO in layered silicates. Intercalation of the polymer chains in the silicate galleries greatly suppresses their tendency to crystallize. The conductivity of PEO/Li⁺-montmorillonite nanocomposite containing 40 wt. % PEO is 1.6×10^{-6} S/cm at 30°C and exhibits a weak temperature dependence with an activation energy of 2.8 kcal/mol. The higher ionic conductivity at ambient temperature compared to conventional LiBF₄/PEO electrolytes combined with their single ionic conductor character makes nanocomposites a promising electrolyte material.

From our studies a new and quite unexpected picture for the nanocomposite electrolytes is emerging. The cations are still pinned to the silicate host surface while the intercalated polymer chains adopt a disordered, random configuration inside the host galleries. Despite the presence of the “confining” host layers, the intercalated PEO chains exhibit substantial segmental motion even at temperatures well below the bulk glass transition of the polymer.

ACKNOWLEDGEMENTS

This work was supported through AFOSR and NSF funding. We would also like to thank our collaborators R. Vaia, B.B. Sauer, R. Krishnamoorti, L. Scanlon, Y.K. Chan and E. Hackett.

REFERENCES

- Aranda, P. and Ruiz-Hitzky, E. (1992) Poly(ethylene oxide)-silicate intercalation materials, *Chem. Mater.*, **4**, 1395-1403.
- Aranda, P. and Ruiz-Hitzky, E. (1994) New polyelectrolyte materials based on smectite polyoxyethylene intercalation compounds, *Acta Polymer.*, **45**, 59-67.
- Boek, E.S., Conevey, P.V., and Skipper, N.T. (1995) Molecular modeling of clay hydration: A study of hysteresis loops in the swelling curves of sodium montmorillonites *Langmuir* **11**, 4629-4631.

- Brindely G.W. and G. Brown, (1980) *Crystal Structure of Clay Minerals and their X-ray Identification*; Mineralogical Society: London, p. 495.
- Cao, G. and Mallouk, T.E. (1991) Topochemical diacetylene polymerization in layered metal phosphate salts *J. Sol. State Chem.*, **94**, 59-71.
- Capuano, F., Core, F., and Scrosati, B. (1991) *J. Electrochem. Soc.*, **138**, 1918.
- Chang, F-R.C., Skipper, N.T. and Sposito, G. (1997) Monte Carlo and molecular dynamics simulations of interfacial structure in lithium-montmorillonite hydrates, *Langmuir* **13**, 2074-2082.
- Deville, A. (1993) *J. Phys. Chem.* **97**, 6261 and 9703.
- Divigalpitiya, W.M.R., Frindt, R.F., and Morrison, S.R. (1991) Molecular composite films of MoS₂ and styrene, *J. Mater. Res.*, **6**, 1103-1107.
- Grim, R.E. (1953) *Clay Mineralogy*, McGraw Hill, New York,
- Hackett, E., Manias, E., and Giannelis, E.P. (1998) Molecular dynamics simulations of organically modified layered silicates. *J. Chem. Phys.* **108**, 7410-7415.
- Hutchinson, J.C., Bissenur, R., and Shriver, D.F. (1996) *Chem. Mater.*, **8**, 1597.
- Kanatzidis, M.G., Marcy, H.O., McCarthy, W.J., Kannewurf, C.R., and Marks, T.J. (1989) In situ intercalative polymerization chemistry of FeOCl - generation and properties of novel, highly conductive inorganic-organic polymer microlaminates, *Solid State Ionics*, **32**, 594-608.
- Kanatzidis, M.G., Wu, C., Marcy, H.O., and Kannewurf, C.R. (1989) Conductive polymer bronzes - intercalated polyaniline in V₂O₅ xerogels, *J. Am. Chem. Soc.*, **111**, 4139-4141.
- Karaborni, S., Smit, B. Heidug, W., and van Oort, E. (1996) The swelling of clays: Molecular simulations of the hydration of montmorillonite, *Science* **271**, 1102-1104.
- Mehrotra, V. and Giannelis, E.P., (1991) Metal-insulator molecular multilayers of electroactive polymers - intercalation of polyaniline in mica-type layered silicates, *Solid State Communications*, **77**, 155-158.
- Messersmith, P.B. and Stupp, S.I. (1992) Synthesis of nanocomposites - organoceramics, *J. Mater. Res.*, **7**, 2599-2611.
- Nazar, L.F., Zhang, Z., and Zinkweg, D. (1992) Insertion of poly(paraphenylenevinylene) in layered MoO₃, *J. Am. Chem. Soc.*, **114**, 6239-6240.
- Pillion, J.E. and Thompson, M.E. (1991) Synthesis and polymerization of propargylamine and aminoacetonitrile intercalation compounds, *Chem. Mater.*, **3**, 777-779.
- Ruiz-Hitzky, E. and Aranda, P. (1990) Polymer-salt intercalation complexes in layer silicates. *Adv. Mater.*, **2**, 545-547.
- Sauer, B.B. and Avakian, P. (1992) Cooperative relaxations in amorphous polymers studied by thermally stimulated current depolarization, *Polymer* **33**, 5128-5142.
- Skaarup, S., West, K., and Zachau-Cristiansen, B. (1980) *B. Solid State Ionics*, **28-30**, 375.
- Skipper; N.T., Chang, F.C., and Sposito G. (1995) Monte-Carlo simulation of interlayer molecular-structure in swelling clay-minerals. 1.

Methodology, *Clay & Clay Minerals*, **43**, 285 -294.

- Vaia, R.A., Vasudevan, S., Krawiec, W., Scanlon, L.G., and Giannelis, E.P. (1995) New polymer electrolyte nanocomposites - melt intercalation of poly(ethylene oxide) in mica-type silicates, *Adv. Mater.* **7**, 154-156.
- Vaia, R.A., Sauer, B.B., Tse O.K., and Giannelis, E.P. (1997) Relaxations of confined chains in polymer nanocomposites: Glass transition properties of poly(ethylene oxide) intercalated in montmorillonite, *J. Polym. Sci.*, **35**, 59-67.
- Wieczorek, W. (1992) Temperature-dependence of conductivity of mixed-phase composite polymer solid electrolytes, *Materials Science and Engineering: B- Solids*, **15**, 108-114.
- Wong, S., Vasudevan, S., Vaia, R.A., Giannelis, E.P., and Zax, D.B. (1995) Dynamics in a confined polymer electrolyte - a Li-7 and H-2 NMR-study, *J. Am. Chem.Soc.*, **117**, 7568-7569.
- Wong, S., Vaia, R.A., Giannelis E.P., and Zax, D.B. (1996) Dynamics in a poly(ethylene oxide)-based nanocomposite polymer electrolyte probed by solid state NMR, *Solid State Ionics*, **86-88**, 547-557.
- Wu, J. and Lerner, M.M. (1993) Structural, thermal, and electrical characterization of layered nanocomposites derived from Na-montmorillonite and polyethers, *Chem. Mater.*, **5**, 835-838.